Vis/NIR hyperspectral imaging technology in predicting the quality properties of three fruit cultivars during production and storage

Alessandro Benelli
Department of Agricultural and Food Sciences
Alma Mater Studiorum, University of Bologna
Cesena, Italy
alessandro.benelli6@unibo.it

Angelo Fabbri
Department of Agricultural and Food Sciences
Alma Mater Studiorum, University of Bologna
Cesena, Italy
angelo.fabbri@unibo.it

***Abstract*—Hyperspectral imaging technology has its origins in the mid-1980s: from hyperspectral cameras developed for remote sensing by aerial vehicles or satellites, the technology has moved to proximal sensing applications on a lab-scale under controlled conditions. In the agri-food sector, hyperspectral imaging technology emerged in the non-destructive measurement of food quality parameters. In recent years, due to the miniaturization of hyperspectral cameras and the increase in computational and data storage capabilities, there is growing interest towards the in-field application of proximal remote sensing hyperspectral cameras mounted on airborne or unmanned aerial vehicles or ground vehicles. As example of the application of the hyperspectral imaging in the agri-food sector, quality attributes (soluble solids content, flesh firmness) of apricots, kiwifruits and grape were monitored by means of a hyperspectral camera, in order to observe their evolution during storage and directly in field.**

Keywords—hyperspectral, apricot, kiwi fruit, grape, flesh firmness, soluble solids content

I. Introduction

The first hyperspectral camera (HSC) was developed in 1984: the Airborne Imaging Spectrometer (AIS) was the first of a new class of high spectral resolution remote sensing instruments, initially employed on a series of geological and vegetational objectives [1]. Subsequently, these instruments were widely used for aerial and satellite remote sensing in the fields of mineralogy, oceanography, environmental and vegetation monitoring, water resources management, precision agriculture [2].

Hyperspectral imaging (HSI) technology combines imaging and spectroscopic technologies, widely used in the food and agriculture sector. While imaging technology is limited to detect external and surface characteristics of samples, HSI technology allows to investigate, due to the integration of spectroscopic technology, some intrinsic chemical and physical characteristics of the sample. Moreover, compared to the traditional spectroscopy, HSI has the advantage to provide a spectrum for each point (voxel) of the acquired HS image, which allows to discriminate the regions of interest (ROIs) from the background [3].

In the last two decades, the use of HSI technology has been extended to controlled environments: the adaptation of HSI technology to proximal sensing allowed its adoption in the medical, forensic, pharmaceutical, biochemical, agricultural, food, recycling, artwork and cultural heritage, and other sectors [2].

With regard to the agro-food sector, HSI technology is currently applied to investigate chemical and physical characteristics of food, which are related to its quality and safety, as moisture content, substances related to proteins, fats, or carbohydrates, texture, color. In the food industry, HSI technology is also applied for the control of food processing, such as thermal processes, freezing, chilling and dehydration of meat, fish, and vegetables. Other applications concern the monitoring of the freshness of meat and fish products; finally, detection defect especially of fruits and vegetables [4].

Fruit in particular has been widely investigated by hyperspectral technology with regard to the prediction of quality attributes, as flesh firmness (FF), soluble solids content (SSC), starch, anthocyanin and moisture content, titratable acidity (TA), pH, color, bruises, chilling injury, pits, apple bitter pits, rotting, citrus fruit canker and fecal contamination [5], [6].

Reference [7] predicted the SSC of two varieties of kiwis, 'Xixuan' and 'Huayou', by means of a near-infrared (NIR) HSI system, operating in the wavelength range of 865.11–1711.71 nm. The best results were obtained from a least square support vector machine (LS-SVM) model, considering the full spectra of the two varieties together, with a correlation coefficient in prediction (R_P) of 0.971, and root-mean-square error of prediction (RMSEP) of 0.589 °Brix (°Bx) [7]. Sugar accumulation was investigated on 'Hayward' kiwifruits in response to a treatment with 1-methylcyclopropene (1-MCP), adopting a visible/near-infrared (Vis/NIR) HSI system, operating in the 400–1000 nm wavelength range. The best performance was obtained on control kiwifruit slices, selecting a maximum of 10 most significant wavelengths through a PLSR model. Concerning glucose and sucrose, a multiple linear regression (MLR) model reached values of determination coefficient in prediction (R^2_P) of 0.934 and 0.705, and RMSEP of 2.04 and 4.37 g kg^{-1} respectively. For fructose, the best prediction results were achieved by applying a LS-SVM model, with values of $R^2_p = 0.867$ and RMSEP = 3.08 g kg^{-1} [8]. A HSI system covering two spectral ranges, 450–1000 nm (Vis/NIR) and 951–1670 nm (NIR), was adopted to predict FF, SSC and pH of three kiwifruit varieties, 'Xuxiang', 'Hongyang', and 'Cuixiang'. A successive projections algorithm–multiple linear regression (SPA-MLR) model performed well at Vis/NIR spectral range for FF and SSC prediction, with $R_P = 0.9812$ and residual prediction deviation (RPD) of 5.17 for SSC, $R_P = 0.9523$ and RPD = 3.26 for FF. RPD consists in the standard deviation of observed values divided by the RMSEP: a good model should have a high RPD, in particular here a RPD ≥ 2.5 was classified and defined as excellent. A genetic algorithm–partial least square–support vector machine (GAPLS-LS-SVM) model was the best one at NIR spectral range for predicting pH, with $R_P = 0.9070$ and RPD = 2.60 [9]. Finally, reference [10]

978-1-7281-8783-9/20/$31.00 ©2020 IEEE

adopted an HSI system operating in the NIR spectral range (1000–1650 nm) on a yellow kiwi cultivar called 'G3'. Principal component analysis (PCA) was applied to the acquired HS images of the external surface and pulp of the kiwis, providing information on the state of ripeness of the fruit [10].

Concerning apricots, reference [11] adopted a Vis/NIR (650–1200 nm) portable spectrometer to evaluate SSC and FF on three apricots varieties, 'Kioto', 'Harostar' and 'Bergarouge'. PLS regression models were built for the three individual apricot varieties and for all the varieties gathered in one data set. The model combining the three varieties gave satisfactory results in the determination of SSC, with a correlation coefficient in calibration (R_C) of 0.90 and root-mean-square error of cross-validation (RMSECV) of 0.67 °Bx. Regarding FF, the best results were obtained for the varieties 'Harostar' and 'Kioto', with R_C of 0.85 and 0.92 and RMSECV of 4.87 and 8.9 DI_{10} (Durofel Index, where the Durofel device adopted for FF measurement was equipped with a 0.10 cm^2 probe) respectively [11]. SSC and FF of apricots cultivar 'Orangered®' were determined by PLS models adopting a portable NIR device (Phazir: 940–1797 nm) to follow up the fruit maturation on tree, obtaining a correlation coefficient in cross-validation (R_{CV}) of 0.66 and root-mean-square error of external validation (RMSEV) of 0.98 °Bx for SSC, and R_{CV} = 0.49 and RMSEV = 5.3 DI for FF. In the second part of the study, 40 apricot cultivars were analyzed in the post-harvest period by means of two portable Vis/NIR instruments (NIR Case: 310–1100 nm; LabSpec®: 350–2500 nm) in order to predict SSC and FF, obtaining, with NIR Case device in the wavelength range 650-970 nm, R_{CV} = 0.95 and RMSECV = 0.58 °Bx for SSC, and R_{CV} = 0.85 and RMSECV = 8.4 DI for FF [12].

SSC of grapes was measured with both spectrometers and HSI systems in the Vis/NIR spectral range. 480 samples of 'Cabernet Sauvignon' wine grape berries were analyzed with a portable Vis/NIR spectrometer (spectral range: 590–1090 nm) to predict SSC by means of PLSR models. The best results in terms of fitting was obtained with a PLSR with variable selection (PLSR-VSEL) model on normalized spectra: the determination coefficient in cross-validation (R^2_{CV}) of 0.72 was the highest, and the standard error of calibration (SEC) and prediction on cross-validation (SEPCV) of 0.53 and 0.61 °Bx respectively were the lowest. Finally, the ratio of standard deviation for the reference values and SEPCV (RPD) was 1.64 [13]. A portable Vis/NIR spectrophotometer (wavelength range: 450–980nm) was built and tested on 156 samples of 'Nebbiolo' grapes. Through PLS models, good statistical parameters for SSC were determined, with R_P = 0.82 and RMSEP = 1.48 [14]. SSC of a 140 berries sample from 7 table grapes cultivars (20 berries for each cultivar) was determined adopting a HSI system, operating in controlled conditions under artificial illumination, and characterized by a 400–1000 nm spectral range. PLSR models were applied, finding good correlations for SSC: for white and red/black grapes the best determination coefficient in validation (R^2_V) was 0.94 and 0.93, with RMSEV of 0.06 and 0.12 °Bx respectively [15].

In recent years, the use of HSI proximal sensing technology directly in the field has become of growing interest to monitor quality attributes of fruit and cereals, fruit ripening, cereals nitrogen content, to detect phenotypes, drought stress, weeds, fungal diseases: however, few works are present in literature [4]. The HSCs have been installed on both airborne or unmanned aerial vehicles (UAV) [16], [17] and ground vehicles [18]–[20].

The present paper aims to introduce the trials carried out during the first two years of the author's PhD. In a controlled environment, quality attributes—soluble solids content (SSC) and flesh firmness (FF)—of apricots and kiwis were evaluated to monitor the evolution of fruit ripening during storage. Finally, the ripening of wine grapes was monitored directly in the field by measuring the SSC of the berries.

II. Hyperspectral Imaging: Operating Principles

A. Hyperspectral camera

A Vis/NIR push-broom linear array HSC (Nano-Hyperspec VNIR, Headwall Photonics, Inc., Fitchburg, MA, USA) was adopted for all the tests performed: the HSC is characterized by the spectral region 400–1000 nm, splitted into 272 spectral bands and with a spectral resolution of 2.2 nm. The optics used has an effective focal length (EFL) of 17 mm, with an angular field of view (FOV) of 15.3°.

The HSC is able to acquire a linear array of 640 voxels. Each voxel is characterized by two spatial and one spectral dimension. To acquire the hyperspectral (HS) image (3D hypercube), it is necessary to move the sample along the scanning direction of the HSC by placing it on a conveyor belt (Fig. 2b and Fig. 3), or to move the HSC, *e.g.* in the case of analysis carried out directly in the field on a UAV or ground vehicle (Fig. 5).

B. Hyperspectral image processing

Before acquiring the HS image, a white and a black reference image should be acquired and subsequently applied to calibrate the HS image. The black image is obtained by covering the lens with the lens cap; the white image should be acquired immediately before the HS image by placing a high reflectance white panel covering the entire FOV of the HSC lens [21].

In order to extract the spectral characteristics and to reduce noise, the resulting spectra should be pre-processed. Through smoothing, wavelength values are averaged over a symmetrically distributed range around a central point: the raw value at this point is replaced by the mean over the range, thus creating a smoothing effect (examples of smoothing techniques: *Savitzky-Golay*, moving average, median filter). In addition, spectra can also be refined: *e.g.* standard normal variate (SNV), derivative, multiplicative scatter correction (MSC), de-trending. To avoid problems of collinearity and also to remove the low signal-to-noise ratio (SNR) bands, it is useful to proceed with the wavelength selection. Examples of wavelength selection techniques are partial least squares regression (PLSR), successive projections algorithm (SPA), stepwise regression (SWR), uninformative variable elimination (UVE). Moreover, wavelength selection contribute to dimensionality reduction of the HS image [21], [22].

To obtain the mean spectrum from the ROIs (Fig. 1), which will be used to build a model, a classification method could be adopted. Among unsupervised classification methods are principal component analysis (PCA), k-means and hierarchical clustering, convolutional neural networks (CNN). Among supervised classification algorithms are soft independent modelling class analogies (SIMCA), partial least

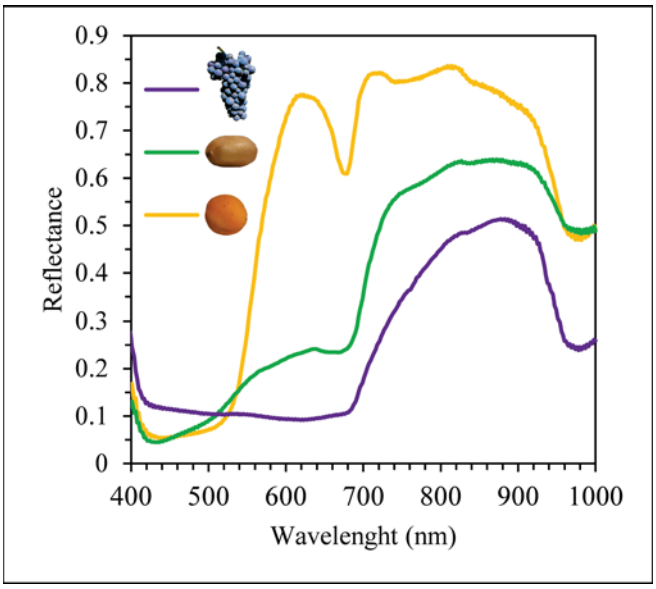

Fig. 1 Raw mean spectra of grapes (purple line), kiwis (green line) and apricots (orange line) samples. The grape spectra were obtained by analyzing grapes directly in the field under natural lighting conditions, those of kiwis and apricots were obtained in the laboratory under artificial light.

square discriminant analysis (PLS-DA), support vector machines (SVMs), k-nearest neighbour (kNN). Finally, regression models are adopted to establish a relationship between HS data and target properties measured in the sample. Linear regression models include multiple linear regression (MLR), principal component regression (PCR), PLSR; non-linear regression models include artificial neural networks (ANN), multilayer perceptron (MLP), generalised regression neural network (GRNN), least squares support vector machines (LS-SVMs) and non-linear PLSR [21].

III. Hyperspectral Imaging of Fruit

A. Stored fruit analysis

1) Apricots

Temperature control is essential to maximize the marketable life of fresh apricots. The shelf life of apricots is short, from 1 to 2 weeks at 0° C and 90% relative humidity, and and they quickly pass from ripeness to over-ripeness [23]. If the apricots are stored at 5–7 °C the texture becomes mealy and the flavour is not retained, while a ripening temperature from 18° to 24 °C is acceptable [24].

The study was conducted on 'Farbaly' apricots analyzed on 9 different days (20 apricots per day). The apricots were stored at 20 °C to simulate fresh market conditions (Fig. 2). FF and SSC were predicted by developing models based on PLS and ANN. Through PLS, the best results were obtained in FF prediction, with $R^2 = 0.85$ in external validation and RMSEP = 1.64 N. Regarding ANN, the best results were obtained in FF prediction, with $R^2 = 0.85$ in test set validation and RMSEP = 1.50.

2) Kiwifruits

Kiwis are harvested when target values for several quality attributes are reached, including FF and SSC, which reflect the physiological maturity of the fruit. SSC, measured with a refractometer, should reach 6.2–6.5 °Bx (9.5 °Bx when introduced into the distribution chain), while FF, measured with an 8 mm probe penetrometer, should be equal to or greater than about 62 N [25], [26]. Commercial maturity

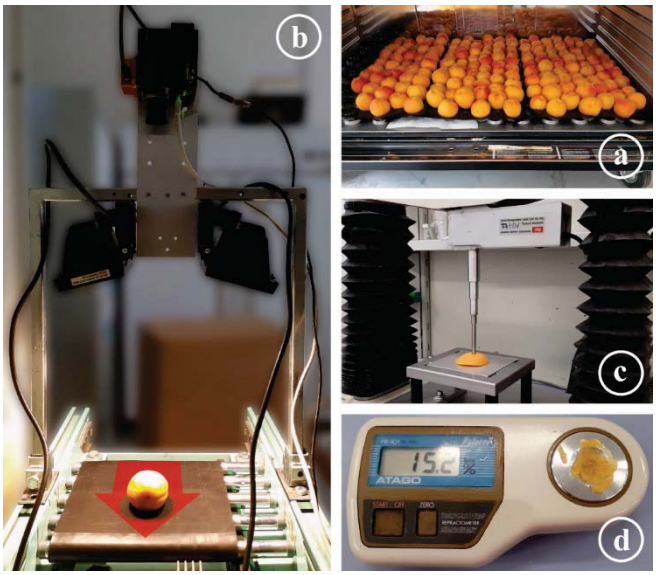

Fig. 2 (a) Apricots were stored at 20 °C to reproduce the fresh market conditions. (b) Lab-scale hyperspectal imaging system adopted for the analysis of the apricots. The red arrow represents the sliding direction of the conveyor belt. (c) Magness-Taylor flesh firmness was determined on each side of the fruit by a compression test performed with a texture analyzer. (d) Soluble solids content was measured by means of a portable digital refractometer.

should finally be reached to satisfy consumer preference: SSC should exceed 12.5 °Bx, while FF should drop below about 9–13 N [26].

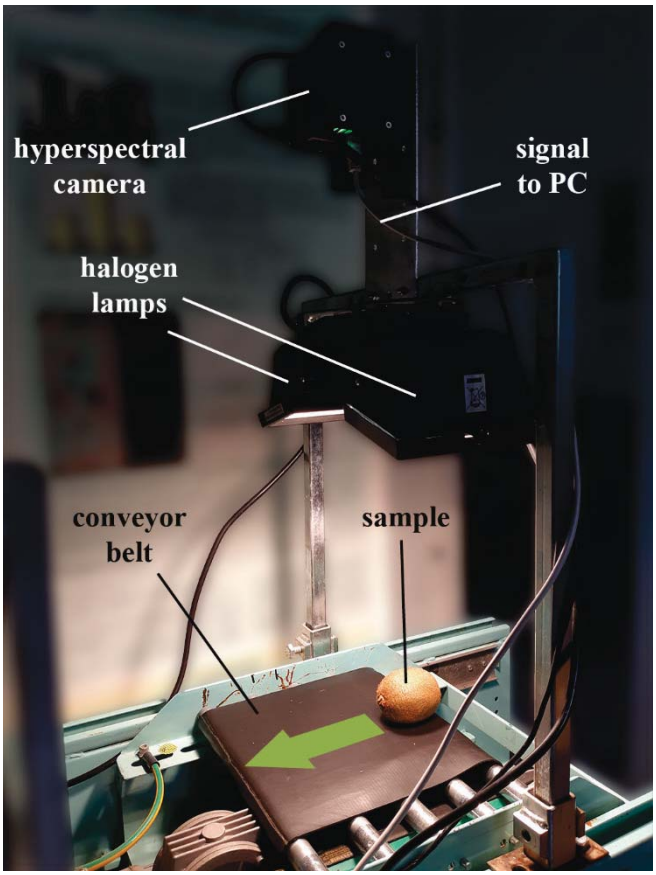

Fig. 3 Lab-scale HSI system adopted for the analysis of kiwis. The green arrow represents the sliding direction of the conveyor belt.

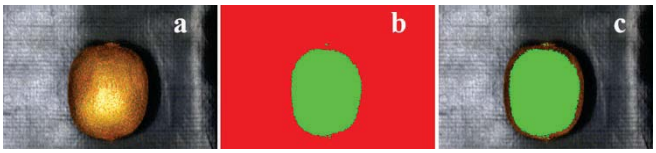

Fig. 4 (a) RGB image obtained from a HSI of a kiwifruit analyzed in a controlled environment with artificial light. (b) Representation in false colors of ROI (green) and background (red) obtained with k-means unsupeervised classification method (number of classes: 2; maximum number of iterations: 30; classification methods: euclidean distance). (c) Overlap of the ROI on (a): the dark edges of the kiwi are not included in the ROI.

130 'Hayward' kiwifruits were analyzed in 5 different days starting from the 2nd day after the harvest, over a period of 36 days (Fig. 3 and Fig. 4). In the first 4 days of analysis 30 samples per day were analyzed, while in the last one the sample was reduced to 10; due to excessive softening many kiwifruits were discarded. FF and SSC were predicted applying PLS based models: the best results were obtained in SSC prediction, with R^2 =0 .91 in cross-validation, and RMSECV = 0.89 °Bx, while for FF R^2 = 0.87 and RMSECV = 11.9 N.

B. In-field analysis of grape ripening

Global climate change has led in recent decades to an increase in the SSC content of grape berries. As a result, the harvest tends to be early, affecting the phenolic and aromatic ripeness, which is not always reached, and the acidity of the grapes tends to decrease. This leads to an increase in the alcohol content of the wine, on the contrary its aging capacity decreases [27]. In an industrialized wine system, it is therefore extremely important to monitor the quality attributes of the grapes in order to control their growth and maturation, and finally to decide when to proceed with the harvest. In this way the prerequisites for obtaining a high-quality wine are defined, with the resulting economic and social impact.

One side of a row of wine grapes (*Vitis vinifera* 'Sangiovese'), located in a vineyard near Cesena (Italy) was analyzed on 13 different days (Fig. 5). The row was divided into 11 sections; for each day of analysis, one hyperspectral image per section was captured. At the same time 3 berries per section were collected to measure the SSC by using a digital refractometer. A predictive model based on PLS was developed, resulting in R^2 = 0.75 in cross-validation, and RMSECV = 0.84 °Bx: these results are similar to those obtained with Vis/NIR portable spectrometers [13], [14].

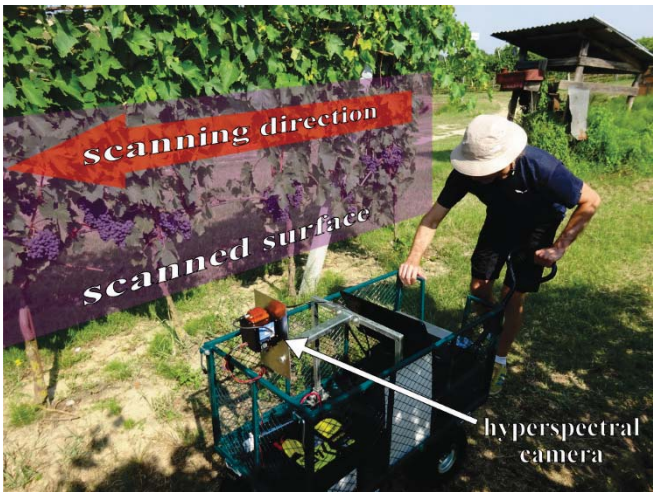

Fig. 5 (a) Vineyard row, highlighted by the purple surface, scanned with the Vis/NIR hyperspectral camera, installed in a cart. The red arrow indicates the scanning direction.

IV. Conclusions

The present studies on apricots and kiwifruits revealed the potential of hyperspectral imaging technology as a lab-scale tool for the non-destructive measurement of fruit quality attributes throughout the whole supply chain. Furthermore, hyperspectral imaging technology has been effective in predicting, directly in the field and under natural light conditions, the soluble solids content of wine grapes in order to monitor the evolution during ripening. The development of hyperspectral image segmentation, selection of regions of interest and spectra processing techniques will be fundamental to carry out on-the-go analysis of large-scale vineyards.

References

[1] G. Vane, A. F. H. Goetz, and J. B. Wellman, "Airborne Imaging Spectrometer: a New Tool for Remote Sensing.," *IEEE Trans. Geosci. Remote Sens.*, vol. GE-22, no. 6, pp. 546–549, 1984, doi: 10.1109/tgrs.1984.6499168.

[2] J. M. Amigo, "Hyperspectral and multispectral imaging: setting the scene," in *Data Handling in Science and Technology*, vol. 32, 2020, pp. 3–16.

[3] B. Park and R. Lu, "Introduction," in *Hyperspectral Imaging Technology in Food and Agriculture*, 2015, pp. 1–390.

[4] A. Benelli, C. Cevoli, and A. Fabbri, "In-field hyperspectral imaging: An overview on the ground-based applications in agriculture," *J. Agric. Eng.*, vol. LI, no. 1030, pp. 129–139, Sep. 2020, doi: 10.4081/jae.2020.1030.

[5] I. Chandrasekaran, S. S. Panigrahi, L. Ravikanth, and C. B. Singh, "Potential of Near-Infrared (NIR) Spectroscopy and Hyperspectral Imaging for Quality and Safety Assessment of Fruits: an Overview," *Food Anal. Methods*, vol. 12, no. 11, pp. 2438–2458, 2019, doi: 10.1007/s12161-019-01609-1.

[6] P. Pathmanaban, B. K. Gnanavel, and S. S. Anandan, "Recent application of imaging techniques for fruit quality assessment," *Trends Food Sci. Technol.*, vol. 94, no. October, pp. 32–42, 2019, doi: 10.1016/j.tifs.2019.10.004.

[7] W. Guo, F. Zhao, and J. Dong, "Nondestructive Measurement of Soluble Solids Content of Kiwifruits Using Near-Infrared Hyperspectral Imaging," *Food Anal. Methods*, vol. 9, no. 1, pp. 38–47, 2016, doi: 10.1007/s12161-015-0165-z.

[8] W. Hu, D. W. Sun, and J. Blasco, "Rapid monitoring 1-MCP-induced modulation of sugars accumulation in ripening 'Hayward' kiwifruit by Vis/NIR hyperspectral imaging," *Postharvest Biol. Technol.*, vol. 125, pp. 168–180, 2017, doi: 10.1016/j.postharvbio.2016.11.001.

[9] H. Zhu, B. Chu, Y. Fan, X. Tao, W. Yin, and Y. He, "Hyperspectral Imaging for Predicting the Internal Quality of Kiwifruits Based on Variable Selection Algorithms and Chemometric Models," *Sci. Rep.*, vol. 7, no. 1, pp. 1–13, 2017, doi: 10.1038/s41598-017-08509-6.

[10] S. Serranti, G. Bonifazi, and V. Luciani, "Non-destructive quality control of kiwi fruits by hyperspectral imaging," 2017, vol. 10217, p. 102170O, doi: 10.1117/12.2255055.

[11] C. Camps and D. Christen, "Non-destructive assessment of apricot fruit quality by portable visible-near infrared spectroscopy," *LWT - Food Sci. Technol.*, vol. 42, no. 6, pp. 1125–1131, 2009, doi: 10.1016/j.lwt.2009.01.015.

[12] D. Christen, C. Camps, A. Summermatter, S. Gabioud Rebeaud, and D. Baumgartner, "Prediction of the pre- and postharvest apricot quality with different VIS/NIRs devices," in *Acta Horticulturae*, 2012, vol. 966, pp. 149–154, doi: 10.17660/actahortic.2012.966.23.

[13] B. Diezma-Iglesias, P. Barreiro, R. Blanco, and F. J. García-Ramos, "Comparison of robust modeling techniques on NIR spectra used to estimate grape quality," in *Acta Horticulturae*, 2008, vol. 802, pp. 367–372, doi: 10.17660/ActaHortic.2008.802.48.

[14] R. Guidetti, R. Beghi, and L. Bodria, "Evaluation of grape quality parameters by a simple VIS/NIR system," in *Transactions of the ASABE*, 2010, vol. 53, no. 2, pp. 477–484.

[15] A. Baiano, C. Terracone, G. Peri, and R. Romaniello, "Application of hyperspectral imaging for prediction of physico-chemical and sensory characteristics of table grapes," *Comput. Electron. Agric.*, vol. 87, pp. 142–151, Sep. 2012, doi: 10.1016/j.compag.2012.06.002.

[16] A. Matese and S. F. Di Gennaro, "Technology in precision viticulture: A state of the art review," *Int. J. Wine Res.*, vol. 7, no. 1, pp. 69–81, 2015, doi: 10.2147/IJWR.S69405.

[17] P. J. Zarco-Tejada, M. L. Guillén-Climent, R. Hernández-Clemente, A. Catalina, M. R. González, and P. Martín, "Estimating leaf carotenoid content in vineyards using high resolution hyperspectral imagery acquired from an unmanned aerial vehicle (UAV)," *Agric. For. Meteorol.*, vol. 171–172, pp. 281–294, 2013, doi: 10.1016/j.agrformet.2012.12.013.

[18] D. Deery, J. Jimenez-Berni, H. Jones, X. Sirault, and R. Furbank, "Proximal remote sensing buggies and potential applications for field-based phenotyping," *Agronomy*, vol. 4, no. 3, pp. 349–379, 2014, doi: 10.3390/agronomy4030349.

[19] A. Wendel, J. Underwood, and K. Walsh, "Maturity estimation of mangoes using hyperspectral imaging from a ground based mobile platform," *Comput. Electron. Agric.*, vol. 155, no. June, pp. 298–313, 2018, doi: 10.1016/j.compag.2018.10.021.

[20] S. Gutiérrez, J. Fernández-Novales, M. P. Diago, and J. Tardaguila, "On-the-go hyperspectral imaging under field conditions and machine learning for the classification of grapevine varieties," *Front. Plant Sci.*, vol. 9, no. July, pp. 1–11, 2018, doi: 10.3389/fpls.2018.01102.

[21] J. Ma, D.-W. Sun, H. Pu, J.-H. Cheng, and Q. Wei, "Advanced Techniques for Hyperspectral Imaging in the Food Industry: Principles and Recent Applications," *Annu. Rev. Food Sci. Technol.*, vol. 10, no. 1, pp. 197–220, 2019, doi: 10.1146/annurev-food-032818-121155.

[22] D. Liu, D.-W. Sun, and X.-A. Zeng, "Recent Advances in Wavelength Selection Techniques for Hyperspectral Image Processing in the Food Industry," *Food Bioprocess Technol.*, vol. 7, no. 2, pp. 307–323, Feb. 2014, doi: 10.1007/s11947-013-1193-6.

[23] P. Rubio and R. Infante, "Preconditioning 'Goldrich' and 'Robada' apricots (Prunus armeniaca L.) harvested at two maturity stages," in *Acta Horticulturae*, 2010, vol. 862, pp. 605–612.

[24] H. Manolopoulou and C. Mallidis, "Storage and processing of apricots," in *Acta Horticulturae*, 1999, vol. 488, no. 488, pp. 567–576, doi: 10.17660/ActaHortic.1999.488.93.

[25] OECD, *Kiwifruit - International Standardisation of Fruit and Vegetables*. OECD, 2008.

[26] C. H. Crisosto and A. A. Kader, "Kiwifruit Postharvest Quality Maintenance Guidelines," Department of Pomology, University of California, Davis, CA 95616, US, 1999.

[27] S. Delrot, H. Medrano, E. Or, L. Bavaresco, and S. Grando, *Methodologies and results in grapevine research*. Springer Netherlands, 2010.